Comparing the kinematics of 2D Euler, Shallow Water Quasi-Geostrophy, and Surface Quasi-Geostrophy using Circular patches of (potential) vorticity.

J.A. Biello

February 9, 2019

1 Introduction

The 2-dimensional Euler equations (E2), Shallow Water Quasi-Geostrophy (SWQG), and Surface Quasi-Geostrophy (SQG) are all theories in two dimensions which describe the transport of a scalar quantity by the incompressible velocity field generated by that scalar. Let

$$u(x,y,t), \quad v(x,y,t) \tag{1}$$

describe a velocity vector field in two spatial dimensions, evolving in time, t. The velocity field will be incompressible,

$$\frac{\partial u}{\partial x} + \frac{\partial v}{\partial y} = 0, \tag{2}$$

which means that it can be described as the *tangential gradient* of a stream function, ψ,

$$u = -\frac{\partial \psi}{\partial y}, \quad v = \frac{\partial \psi}{\partial x}. \tag{3}$$

Let us use

$$q(x,y,t) \tag{4}$$

to represent the scalar quantity which is transported in each of these theories. Its dynamics are given by the transport equation,

$$\frac{Dq}{Dt} = 0, \quad \text{where} \quad \frac{D}{Dt} = \frac{\partial}{\partial t} + u\frac{\partial}{\partial x} + v\frac{\partial}{\partial y}. \tag{5}$$

The physical meaning of q differs according to which theory we are discussing. In 2-d Euler (E2), q is the vorticity (i.e. the curl of the velocity field). Therefore it is related to the stream function through

$$q = \Delta\psi \qquad \text{(E2)} \tag{6}$$

where $\varDelta$ is the 2-dimensional Laplacian operator

$$\varDelta = \frac{\partial^2}{\partial x^2} + \frac{\partial^2}{\partial y^2}. \tag{7}$$

In the shallow water quasi-geostrophic theory (SWQG), q is the potential vorticity (see Vallis's book) and is related to the stream function through

$$q = \varDelta\psi - \frac{\psi}{L^2} + f(y). \qquad \text{(SWQG)} \tag{8}$$

In the QG theory, $L = \frac{c}{f(0)}$ is called the deformation length scale, where c is the gravity wave speed and $f(y)$ is the planetary rotation rate as a function of the meridional coordinate, y.

The surface quasi-geostrophic theory is derived from 3-dimensional quasi-geostrophy by assuming a temperature jump as a function of (x, y), but at a fixed height, z. This yields a potential vorticity (PV) which is singular at the height of the jump and zero elsewhere - a potential vorticity sheet. In this theory, $q(x, y)$ plays the role of the temperature jump and it is related to the stream function through the square root of the Laplacian operator

$$q = -\left(-\varDelta\right)^{\frac{1}{2}}\psi \quad \text{(SQG)}. \tag{9}$$

The stream function can be expressed as on of the Riesz transforms of q.

Notice that E2 and SQG can be seen as a two members of a family of theories where different powers of the Laplacian relate the stream function to the scalar. J.K. Hunter is studying some of these generalizations. Also notice that SWQG is the only one of these three theories that has a length scale in the problem, L.

In this note, I will construct the stream function for these three theories in the case where the scalar is a δ-distribution and when it is constant within a circular patch. For SWQG I will focus on f is constant, so the additive f (so called planetary PV) is not relevant to the solution. The objective is to compare and contrast the kinematic properties of these flow fields in order to begin to visualize how they would evolve under the dynamics.

2 2-d Euler circular patch

This is a straightforward classical result - it is something basic we teach in an introductory partial differential equations class, for example. The vorticity is related to the stream function through

$$\varDelta\psi = q \tag{10}$$

where $q = q_0$ on $r \leq a$ and $q = 0$ elsewhere (r is the polar coordinate). Integrating over a disk of radius R center on the origin, we find

$$\begin{aligned}
\int_0^R \int_0^{2\pi} \frac{1}{r}\frac{\partial}{\partial r}\left[r\frac{\partial\psi}{\partial r}\right]\ r\,d\theta dr &= \int_0^R \int_0^{2\pi} q_0\,\chi_{[0,a]}(r)\ \ r\,d\theta dr \\
R\frac{\partial\psi}{\partial R} &= q_0 \left\{ \begin{array}{ll} \frac{R^2}{2} & R < a \\ \frac{a^2}{2} & R \geq a \end{array} \right. \\
\frac{\partial\psi}{\partial r} &= \frac{q_0}{2} \left\{ \begin{array}{ll} r & r < a \\ \frac{a^2}{r} & r \geq a \end{array} \right. \\
\psi &= \frac{q_0 a^2}{4} \left\{ \begin{array}{ll} \left[\frac{r}{a}\right]^2 & r < a \\ 2\ln\left[\frac{r}{a}\right] + 1 & r \geq a. \end{array} \right.
\end{aligned} \tag{11}$$

The vortex patch has a stream function which grows quadratically with distance from the origin for points within the vortex patch and logarithmically with distance for points outside the vortex patch. The velocity, $\frac{\partial\psi}{\partial r}$ grows linearly with distance inside the patch and decays with distance outside the patch. The stream function and velocity as a function of distance

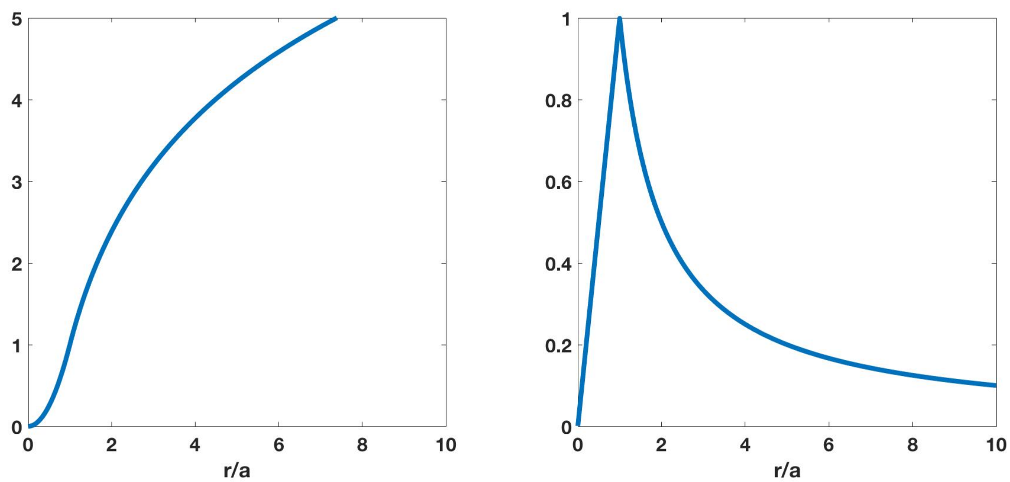

Figure 1: Stream function, ψ, (left) and angular velocity, ψ_r, (right) versus distance from the center of a vortex patch in 2-dimensional euler. The velocity is linear as a function of distance from center within the vortex patch, and decays with distance to the power of one outside.

are plotted in figure 1.

2.1 The Green's function for E2

We should just record the solution of the Green's function for E2. Solve

$$\Delta\psi = \alpha\,\delta^2(\vec{x}) \tag{12}$$

by integrating over a disk of radius R and using the fact that the integral of the delta distribution is equal to one over this area,

$$2\pi R \frac{\partial \psi}{\partial R} = \alpha \tag{13}$$

which shows that

$$\frac{\partial \psi}{\partial r} = \frac{\alpha}{2\pi r}, \quad \Longrightarrow \quad \psi = \frac{\alpha}{2\pi} \ln(r). \tag{14}$$

Since the integration constant for ψ is arbitrary, we have set it to zero for the Green's function. Notice that this result matches the circular patch velocity if we replace

$$q_0 \, \pi a^2 \to \alpha \tag{15}$$

and let

$$a \to 0 \tag{16}$$

with α finite (nonzero).

2.2 What does this mean?

Circular vortex patches in E2 are stable to perturbations. In fact, the largest scale regular perturbation, an ellipse of constant vorticity, is an exact, rotating solution. This is called the Kirchoff vortex. This stability is due to the particular structure of the vortex velocity field near the boundar of the vortex, where it behaves as the absolute value of distance from the boundary. This makes E2 vortex patches somewhat robust.

3 Shallow water quasi-geostrophy circular patch

SWQG is the only one of these examples with an intrinsic length scale, L. Therefore we will have to consider examples with $a > L$ and $a < L$ - where a is the radius of the patch.

3.1 The Green's function for SWQG

The way to approach this problem is to solve

$$\nabla^2 \psi' - \frac{\psi'}{L^2} = \alpha \delta^2(\vec{x}) \tag{17}$$

for ψ'. Seeking circularly symmetric solutions we write

$$\frac{1}{r} \frac{\partial}{\partial r} \left[r \frac{\partial \psi'}{\partial r} \right] - \frac{\psi'}{L^2} = \alpha \delta^2(\vec{x}). \tag{18}$$

The solution to the homogeneous problem is the modified Bessel function of the second kind $K_0(s)$, i.e.

$$\psi'(r,\theta) = A\, K_0\left(\frac{r}{L}\right) \tag{19}$$

The amplitude, A, is determined by integrating around the δ distribution over a disk of radius R and taking the limit as $R \to 0$

$$\begin{aligned} \lim_{R\to 0} \int\int_{\mathrm{Disk_R}} \left[\nabla\cdot\nabla\psi' - \frac{\psi'}{L^2}\right] dA = \int\int_{\mathrm{Disk_R}} \alpha\delta^2 dA \\ \lim_{R\to 0} \int_{\mathrm{Circle_R}} \frac{\partial\psi'}{\partial r} R d\theta = \alpha \\ \lim_{R\to 0} 2\pi A \frac{R}{L}\left.\frac{dK_0}{ds}\right|_{s=\frac{R}{L}} = \alpha \end{aligned} \tag{20}$$

The asymptotics of the modified Bessel function for small argument is

$$\lim_{s\to 0} K_0(s) = -\log(s) - \gamma \tag{21}$$

where γ is the Euler-Mascheroni constant $\gamma = 0.57721\ 56649\ ...$ (which is not actually needed to determine the amplitude, A). Using this limit we find

$$A = -\frac{\alpha}{2\pi}, \tag{22}$$

which is the same as amplitude in E2, since the functional forms of the solution have the same limit as the distance from the delta distribution goes to zero. We conclude that the stream function for a point source in SWQG is

$$\psi = -\frac{\alpha}{2\pi}\, K\left(\frac{r}{L}\right). \tag{23}$$

In order to understand the behavior of SWQG at large distances from a source, we need the asymptotics of the modified Bessel function in the limit of large distance

$$K_0(s) \sim \sqrt{\frac{\pi}{2s}}\, e^{-s}\left[1 - \frac{1}{8s} + \frac{9}{2!\ (8s)^2} + ...\right]. \tag{24}$$

The Bessel function drops off exponentially with distance from the origin, meaning that the velocity field it induces also drops off exponentially. Therefore SWQG has a much more limited range than either E2 or SQG (as we will show in the next section). This exponential drop off will also persist in the case of the circular patch, outside of the patch.

3.2 Circular patch for SWQG

We now solve for the stream function from a circular patch of constant potential vorticity (PV) in SWQG, with zero PV outside the patch,

$$\Delta\psi - \frac{\psi}{L^2} = q \tag{25}$$

where $q = q_0$ on $r \leq a$ and $q = 0$ elsewhere (r is the polar coordinate). In order to compute this solution we have to convolve the Green's function with the source function, q - the most straightforward way to do this is to take the Fourier transform. First, define the wavenumber in polar coordinates

$$\vec{k} = \kappa\left[\cos(\lambda)\hat{\imath} + \sin(\lambda)\hat{\jmath}\right]. \tag{26}$$

Taking the 2-D Fourier transform of both sides of (25) yields

$$\begin{aligned}
-\left(\kappa^2 + L^{-2}\right)\,\tilde{\psi}(\kappa,\lambda) &= q_0 \int_0^a \int_0^{2\pi} e^{-i\kappa r\cos(\theta-\lambda)}\; r dr\, d\theta \\
&= 2\pi q_0 \int_0^a J_0\left(\kappa r\right)\; r\, dr \\
\tilde{\psi}(\kappa,\lambda) &= -\frac{2\pi q_0}{\kappa^2 + L^{-2}} \int_0^a J_0\left(\kappa r\right)\; r\, dr \\
&= -\frac{2\pi q_0}{\kappa^2\left[\kappa^2 + L^{-2}\right]} \int_0^{\kappa a} J_0\left(s\right)\; s\, ds
\end{aligned} \tag{27}$$

which is independent of λ since the patch is circularly symmetric.

The Bessel function satisfies the relation

$$\left[\frac{1}{x}\frac{d}{dx}\right]^m \left[x^n J_n(x)\right] = x^{n-m}\, J_{n-m}(x). \tag{28}$$

Letting $n = m = 1$ we find

$$\begin{aligned}
\frac{1}{x}\frac{d}{dx}\left[xJ_1\right] &= J_0 \\
J_1(x) &= \frac{1}{x}\int_0^x J_0(s)\; sds
\end{aligned} \tag{29}$$

Substitute into $\tilde{\psi}$ to find

$$\tilde{\psi}(\kappa,\lambda) = -\frac{2\pi a q_0}{\kappa\left[\kappa^2 + L^{-2}\right]}\; J_1(\kappa a). \tag{30}$$

Inverting the Fourier transform

$$
\begin{aligned}
\psi\left(r,\theta\right) &= \frac{1}{\left(2\pi\right)^{2}}\int_{0}^{2\pi}\int_{0}^{\infty}\tilde{\psi}(\kappa,\lambda)e^{i\kappa r\,\cos(\lambda-\theta)}\ \kappa d\kappa d\lambda \\
&= -\frac{aq_{0}}{2\pi}\int_{0}^{2\pi}\int_{0}^{\infty}e^{i\kappa r\cos(\lambda)}\ \frac{J_{1}(\kappa a)}{\kappa\left[\kappa^{2}+L^{-2}\right]}\ \kappa\, d\kappa\, d\lambda \\
&= -aq_{0}\int_{0}^{\infty}\frac{J_{0}\left(\kappa r\right)\ J_{1}\left(\kappa a\right)}{\left[\kappa^{2}+L^{-2}\right]}\ d\kappa.
\end{aligned}
\tag{31}
$$

Now we rewrite this expression by letting $\kappa a = s$ and adding a (yet to be determined) constant so that ψ vanishes at the origin

$$
\begin{aligned}
\psi(r,\theta) &= c - aq_{0}\int_{0}^{\infty}\frac{J_{0}\left(s\frac{r}{a}\right)\ J_{1}\left(s\right)}{\left[\left(\frac{s}{a}\right)^{2}+L^{-2}\right]}\ \frac{ds}{a} \\
&= q_{0}a^{2}\left[C-\int_{0}^{\infty}\frac{J_{0}\left(s\frac{r}{a}\right)\ J_{1}\left(s\right)}{\left[s^{2}+\left(\frac{a}{L}\right)^{2}\right]}\ ds\right] \\
&= q_{0}a^{2}\int_{0}^{\infty}\frac{\left[1-J_{0}\left(s\frac{r}{a}\right)\right]\ J_{1}\left(s\right)}{\left[s^{2}+\left(\frac{a}{L}\right)^{2}\right]}\ ds
\end{aligned}
\tag{32}
$$

where I have used the fact that $J_0(0) = 1$ to implicitly determine the constant C. We see that this integral vanishes at $r = 0$ (as required). As $s \to 0$ the integrand remains regular since $J_1(s) \propto s$ there. As $s \to \infty$, $J_0, J_1 \propto s^{-\frac{1}{2}}$ so the integrand is proportional to $s \propto s^{-\frac{5}{2}}$, so is integrable. Therefore, we expect the function to have no singularities as long as L remains finite. In the limit $L \to \infty$ we expect the result from SWQG to match that of E2.

I will perform this integral numerically for the different regimes in the following subsections.

3.3 Large deformation radius (equivalently, small patches), $L \gg a$

For this case we use $L = 10a$ and plot the stream function integral in figure 2. The stream function is plotted in the top left frame. The velocity as a function of r/a is plotted on the top right. On the bottom left is a log-log plot of the velocity (in blue) along with the line r^{-1} (in green) for comparison. It shows that within the patch, the velocity increases linearly in r (solid body rotation) and decreases as r^{-1} just beyond the edge of the patch. On the bottom right is a log-linear plot of the velocity (in blue) for larger distances from the patch (up to $r/a = 100$) with the line $10^{-\frac{r+12.5}{22.5}}$ for comparison. This shows that the velocity decays exponentially at large distances from the patch, as we expect from the Green's function.

In this limit the PV patch rotates almost exactly as a solid body and the velocity close to, but outside the patch, behaves as the velocity of a vortex in 2-dimensional Euler. This would suggest that a PV patch with radius much less than the deformation radius would

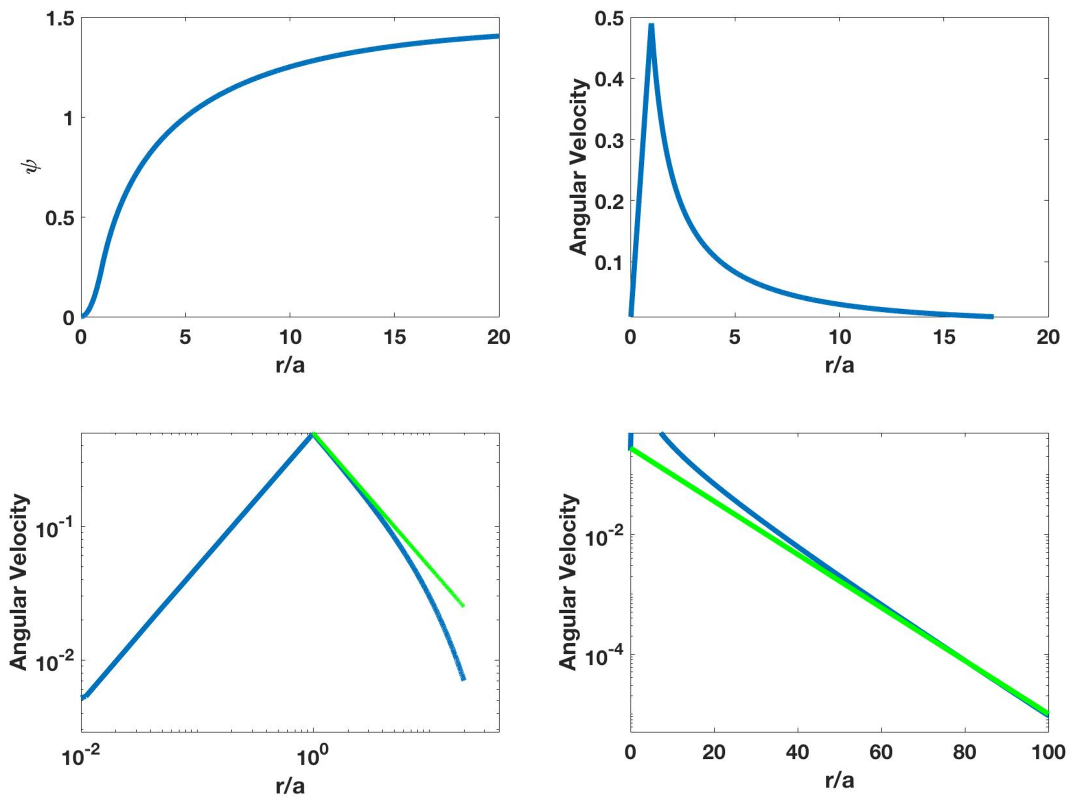

Figure 2: The SWQG theory when L is large, $L = 10a$. The stream function is plotted in the top left frame. The velocity as a function of r/a is plotted on the top right. On the bottom left is a log-log plot of the velocity (in blue) along with the line r^{-1} (in green) for comparison. It shows that within the patch, the velocity increases linearly in r (solid body rotation) and decreases as r^{-1} just beyond the edge of the patch. On the bottom right is a log-linear plot of the velocity (in blue) for larger distances from the patch (up to $r/a = 100$) with the line $10^{-\frac{r+12.5}{22.5}}$ for comparison. This shows that the velocity decays exponentially at large distances from the patch, as we expect from the Green's function.

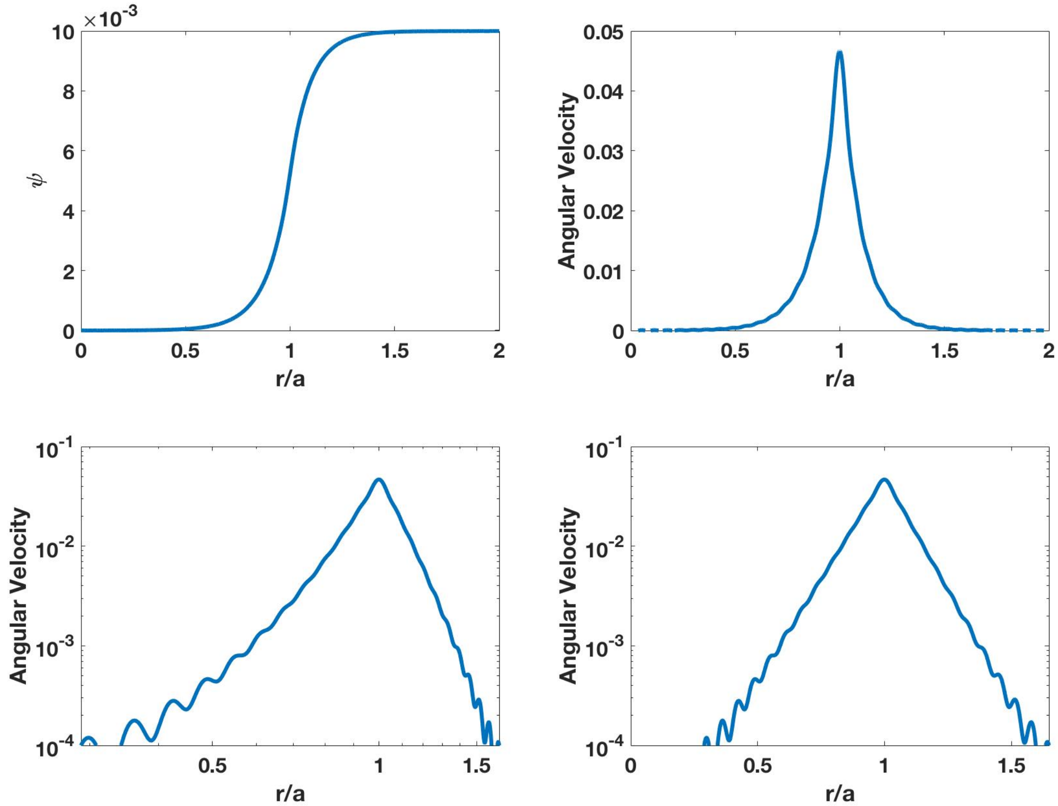

Figure 3: The SWQG theory when L is small, $L = a/10$. The stream function is plotted in the top left frame, the velocity is plotted on the top right, on the bottom left is a log-log plot of the velocity, and on the bottom right is a log-linear plot of the velocity.

behave similar to E2 in this limit - i.e. an isolated patch would remain stable and we could even expect PV elliptical patches to be nearly exact rotating solutions.

3.4 Small deformation radius (equivalently large patches), $L \ll a$

For this case we use $L = a/10$ and plot the stream function integral in figure 3. The stream function is plotted in the top left frame, the velocity is plotted on the top right, on the bottom left is a log-log plot of the velocity, and on the bottom right is a log-linear plot of the velocity.

It is clear from the figures that the stream function looks nothing like the other cases, and in fact the velocity field exponentially decays around the boundary of the patch. This is a fascinating result with respect to the stability of large patches. The shear is very strong there and we would expect shear instabilities to act quickly to destroy large PV patches.

3.5 An analytic solution for an SWQG patch using the Green's function

Since we seek circularly symmetric solutions of SWQG we can convert the equation to an ODE, and take the derivative of both sides of the equation

$$\begin{aligned}
\frac{1}{r}\frac{d}{dr}\left[r\frac{d\psi}{dr}\right] - \frac{\psi}{L^2} &= q \\
\frac{d}{dr}\left[\frac{1}{r}\frac{d(rv)}{dr}\right] - \frac{v}{L^2} &= -q_0\delta(r-a) \\
\frac{d}{dr}\left[\frac{1}{r}\left[v + rv'\right]\right] - \frac{v}{L^2} &= -q_0\delta(r-a) \\
v'' + \frac{v'}{r} - \frac{v}{r^2} - \frac{v}{L^2} &= -q_0\delta(r-a) \\
r^2\frac{d^2v}{dr^2} + r\frac{dv}{dr} - v\left[1 + \frac{r^2}{L^2}\right] &= -q_0\, r^2\, \delta(r-a) \\
s^2\frac{d^2v}{ds^2} + s\frac{dv}{ds} - v\left[1 + s^2\right] &= -q_0\, L^2\, s^2\, \delta(Ls-a)
\end{aligned} \tag{33}$$

The way to think of this equation is that

$$s^2\frac{d^2v}{ds^2} + s\frac{dv}{ds} - v\left[1 + s^2\right] = 0 \tag{34}$$

away from the boundary of the patch ($s = \frac{a}{L}$). The jump in the velocity is determined by integrating over the boundary of the patch

$$\begin{aligned}
\left[\frac{dv}{ds}\right]\Bigg|_{s=\frac{a}{L}} &= -q_0L^2\int_{\frac{a}{L}-\epsilon}^{\frac{a}{L}+\epsilon} \delta(Ls-a)\, ds \\
&= -q_0L\int_{a-\epsilon L}^{a+\epsilon L} \delta(r-a)\, dr \\
\left[\frac{dv}{ds}\right]\Bigg|_{s=\frac{a}{L}} &= -q_0L \\
\left[\frac{dv}{dr}\right]\Bigg|_{r=a} &= -q_0
\end{aligned} \tag{35}$$

The solution to this equation are the modified Bessel functions of the first and second kind $I_1(s), K_1(s)$. Since the former is singular at infinity and the latter is singular at zero, we can write

$$v\left(r\right) = q_0\lambda \begin{cases} \frac{I_1\left(\frac{r}{L}\right)}{I_1\left(\frac{a}{L}\right)} & r < a \\ \frac{K_1\left(\frac{r}{L}\right)}{K_1\left(\frac{a}{L}\right)} & r > a. \end{cases} \tag{36}$$

This form ensures that the velocity is continuous at $r = a$ and its amplitude is proportional to q_0. The parameter λ is determined by the jump condition, and is the solution to

$$\lambda \left[\frac{I_1' \left(\frac{a}{L} \right)}{I_1 \left(\frac{a}{L} \right)} - \frac{K_1' \left(\frac{a}{L} \right)}{K_1 \left(\frac{a}{L} \right)} \right] = L. \tag{37}$$

In order to solve for λ it is convenient to replace the derivatives of the Bessel function with Bessel functions - since this can be done with the derivative recurrence relations

$$\begin{aligned} \frac{dI_1(s)}{ds} &= \frac{I_0(s) + I_2(s)}{2} \\ \frac{dK_1(s)}{ds} &= -\frac{K_0(s) + K_2(s)}{2}. \end{aligned} \tag{38}$$

For ease of notation, let $s = \frac{a}{L}$ again and $\Lambda = \frac{\lambda}{L}$, to find the relation

$$\Lambda(s) = 2 \left[\frac{I_0(s) + I_2(s)}{I_1(s)} + \frac{K_0(s) + K_2(s)}{K_1(s)} \right]^{-1}. \tag{39}$$

The solution $\Lambda(s)$ is plotted on a log-log plot in figure 4 along with a fit $\frac{s}{2}$ in red ($s = \frac{a}{L}$). The plot indicates that the fit is excellent for $s < 1$ and that $\Lambda = \frac{1}{2}$ is the fit for $s > 1$.

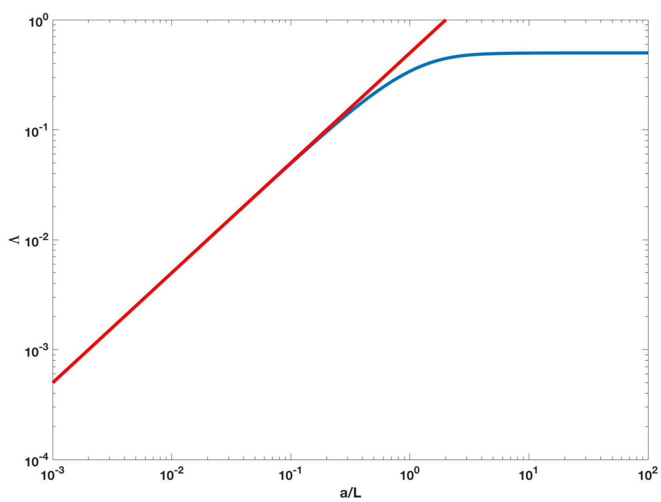

Figure 4: Log-log plot of $\Lambda(s)$ in blue with a fit $\frac{s}{2}$ in red ($s = \frac{a}{L}$). The plot indicates that the fit is excellent for $s < 1$ and that $\Lambda = \frac{1}{2}$ is the fit for $s > 1$.

3.5.1 Using the analytic solution when $\frac{a}{L} \gg 1$

In the large patch regime we have $\Lambda \approx \frac{1}{2}$ so that $\lambda = \frac{L}{2}$. We can use the asymptotics of Bessel functions of large argument, i.e.

$$I_1(s) = \frac{e^s}{\sqrt{2\pi s}}, \quad K_1(s) = \sqrt{\frac{\pi}{2s}} e^{-s}. \tag{40}$$

Substituting this into the expression for (36) we find

$$\frac{I_1\left(\frac{r}{L}\right)}{I_1\left(\frac{a}{L}\right)} = \sqrt{\frac{a}{r}}\, e^{\frac{r-a}{L}} \tag{41}$$

and

$$\frac{K_1\left(\frac{r}{L}\right)}{K_1\left(\frac{a}{L}\right)} = \sqrt{\frac{a}{r}}\, e^{-\frac{r-a}{L}} \tag{42}$$

so that the velocity field is

$$v(r) = \frac{q_0 L}{2}\sqrt{\frac{a}{r}}\, e^{-\left|\frac{r-a}{L}\right|}. \tag{43}$$

This is a very nice analytic expression which agrees with the numerical result we found above near $r = a$.

Near the center of a large patch we have $r \ll L$ but $a \gg L$.

$$\begin{aligned} v(r) &= \frac{q_0 L}{2}\,\frac{I_1\left(\frac{r}{L}\right)}{I_1\left(\frac{a}{L}\right)} \\ &= \frac{q_0 L}{2}\,\left[\frac{r}{2L}\right]\left[\sqrt{2\pi\frac{a}{L}}\, e^{-\frac{a}{L}}\right] \\ &= q_0\sqrt{\frac{\pi}{8}}\,\sqrt{\frac{a}{L}} e^{-\frac{a}{L}}\, r \end{aligned} \tag{44}$$

Near the origin, the patch rotates as a solid body with a shear of

$$q_0\sqrt{\frac{\pi}{8}}\,\sqrt{\frac{a}{L}} e^{-\frac{a}{L}} \tag{45}$$

which is much less than q_0 since $a \gg L$.

3.5.2 Using the analytic solution when $\frac{a}{L} \ll 1$

In this limit $\Lambda = \frac{s}{2}$, so that $\lambda = \frac{a}{2}$. For small argument, the modified Bessel functions are

$$\frac{I_1\left(\frac{r}{L}\right)}{I_1\left(\frac{a}{L}\right)} = \frac{r}{a} \tag{46}$$

and

$$\frac{K_1\left(\frac{r}{L}\right)}{K_1\left(\frac{a}{L}\right)} = \frac{a}{r}. \tag{47}$$

Therefore the velocity field is

$$v(r) = \frac{q_0 a}{2}\left[\frac{r}{a}\right]^n \tag{48}$$

where $n = 1$ for $r < a$, $n = -1$ for $r \geq a$. This expression is valid for $r < L$ since the Bessel function $K_1(s)$ will exhibit exponentially decaying behavior for $r > L$. In the interior (near the origin) the patch rotates as a solid body with a shear of

$$\frac{q_0}{2}. \tag{49}$$

Compare this to the result of a large patch above and we see that a small patch rotates much more rapidly.

These two analytic results - in the limit of large and small patches, also yield more information. Notice that the maximum angular velocity always occurs at $r = a$, the boundary of the patch. Consider a fixed deformation scale, L, (i.e. a fixed planet or a fixed experimental setup) and a fixed potential vorticity, q_0. Patches which are smaller than this scale, $a < L$, have a maximum speed which grows linearly with their radius. Patches which are larger than this scale have a maximum speed which is independent of radius.

4 SQG circular patch

We now solve for the stream function from a circular temperature patch of constant temperature in SQG, with zero temperature outside the patch,

$$-\left(-\Delta\right)^{\frac{1}{2}}\psi = q \tag{50}$$

where $q = q_0$ on $r \leq a$ and $q = 0$ elsewhere (r is the polar coordinate). Define the wavenumber in polar coordinates as,

$$\vec{k} = \kappa\left[\cos(\lambda)\hat{i} + \sin(\lambda)\hat{j}\right] \tag{51}$$

and taking the 2-D Fourier transform of both sides yields

$$\begin{aligned}
-\kappa\tilde{\psi}(\kappa,\lambda) &= q_0\int_0^a\int_0^{2\pi} e^{-i\kappa r\cos(\theta-\lambda)}\; r dr\, d\theta \\
&= 2\pi q_0\int_0^a J_0\left(\kappa r\right)\; r\, dr \\
\tilde{\psi}(\kappa,\lambda) &= -\frac{2\pi q_0}{\kappa}\int_0^a J_0\left(\kappa r\right)\; r\, dr \\
&= -\frac{2\pi q_0}{\kappa^3}\int_0^{\kappa a} J_0\left(s\right)\; s\, ds
\end{aligned} \tag{52}$$

The Bessel function satisfies the relation

$$\left[\frac{1}{x}\frac{d}{dx}\right]^m [x^n J_n(x)] = x^{n-m}\, J_{n-m}(x). \tag{53}$$

Letting $n = m = 1$ we find

$$\begin{aligned} \frac{1}{x}\frac{d}{dx}\,[xJ_1] &= J_0 \\ J_1(x) &= \frac{1}{x}\int_0^x J_0(s)\; sds \end{aligned} \tag{54}$$

Substitute into $\tilde{\psi}$ to find

$$\tilde{\psi}(\kappa, \lambda) = -\frac{2\pi a q_0}{\kappa^2}\; J_1(\kappa a). \tag{55}$$

Inverting the Fourier transform

$$\begin{aligned} \psi\,(r,\theta) &= \frac{1}{(2\pi)^2}\int_0^{2\pi}\int_0^{\infty} \tilde{\psi}(\kappa,\lambda) e^{i\kappa r\, \cos(\lambda-\theta)}\; \kappa d\kappa d\lambda \\ &= -\frac{a q_0}{2\pi}\int_0^{2\pi}\int_0^{\infty} e^{i\kappa r \cos(\lambda)}\; \frac{J_1(\kappa a)}{\kappa^2}\; \kappa\, d\kappa\, d\lambda \\ &= -a q_0 \int_0^{\infty} \frac{J_0\,(\kappa r)\;\, J_1\,(\kappa a)}{\kappa}\; d\kappa. \end{aligned} \tag{56}$$

Now we rewrite this expression by letting $\kappa a \to \kappa$ and adding a constant so that ψ vanishes at the origin

$$\psi(r,\theta) = F\left(\frac{r}{a}\right) = a q_0 \left[1 - \int_0^{\infty} \frac{J_0\left(\kappa \frac{r}{a}\right)\; J_1\,(\kappa)}{\kappa}\; d\kappa\right]. \tag{57}$$

We could explore limits and the like, but it is straightforward to evaluate this integral numerically.

In Figure 5 is plotted the function in parenthesis of equation (57) - the stream function for an SQG patch - versus distance from the origin, $\frac{r}{a}$. The function is quadratic near the origin, and behaves as $1 - \left(\frac{a}{r}\right)$ for $r \gg a$. The angular velocity is plotted in figure 6. It shows that the patch rotates as a solid body at small distances, has a logarithmic singularity in its velocity at the boundary of the patch, and then decays as r^{-2} at large distances. This decay is more rapid than that of either E2 or SWGQ.

5 What does this all mean?

The basic conclusion is that, since E2 has solid body rotation within the patch and a reciprocal distance decay outside the patch, circular patches are stable - as are elliptical patches. SQG has a very singular velocity field at the boundary of the patch. SWQG behaves like

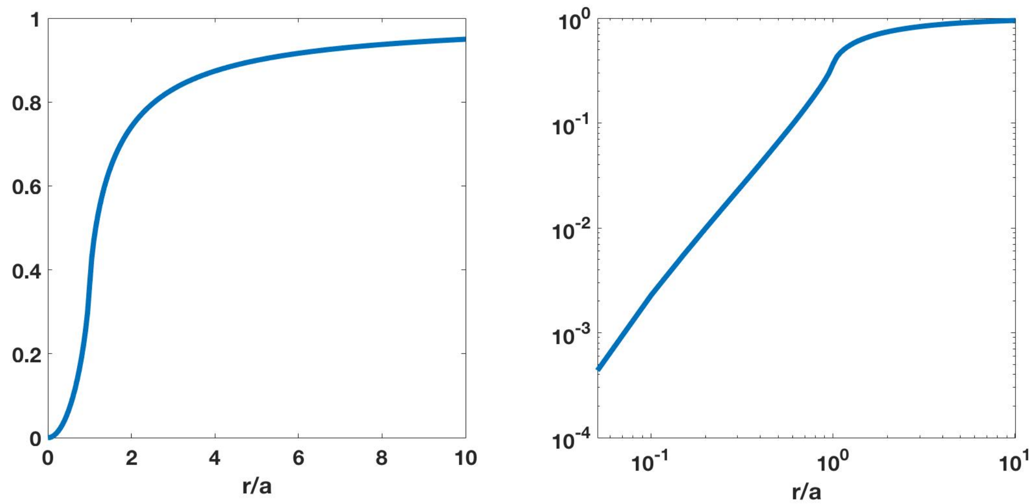

Figure 5: Scaled version of the stream function versus scaled distance from origin for a circular SQG patch. Left plot is linear, right plot is log-log. Notice that the derivative becomes infinite at $r = a$. The function behaves as $1 - \left(\frac{a}{r}\right)$ for $r \gg a$.

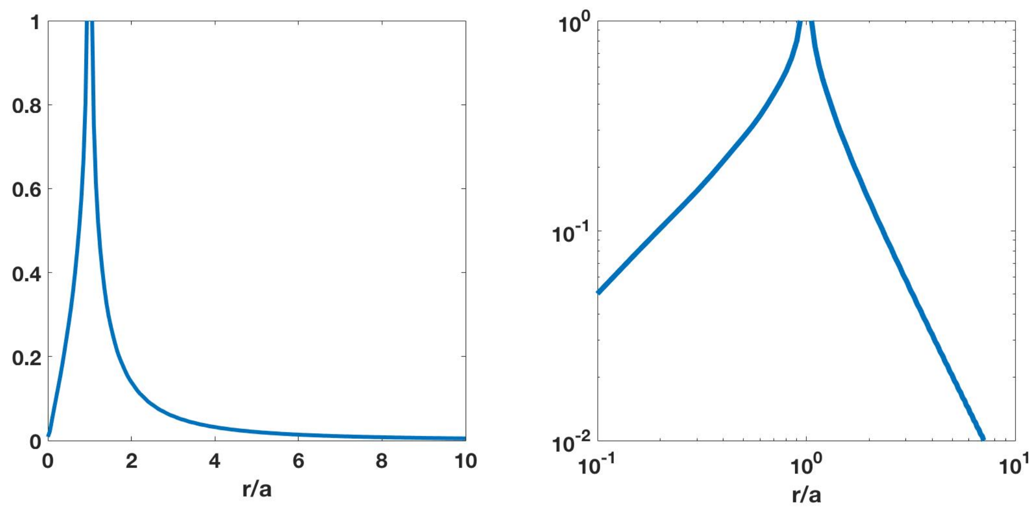

Figure 6: Angular velocity, ψ_r, versus distance from the center of the patch - left is linear, right is log-log. The velocity is linear as a function of distance from center for small distances - which means that it limits to solid body rotation. Near the boundary, the velocity is logarithmically singular. At large distances, the velocity drops off as r^{-2}, more rapid than E2 or SWQG.

E2 for small patches and has a very strong shear for large patches. I believe that this strong shear makes any patches which are larger than the deformation radius, L, susceptible to strong shears if perturbed, and therefore they become unstable under their self-induced velocity field.

6 Adding the β effect to a circular patch

I'll begin with the so-called barotropic QG theory. The advection equation for the total PV reads

$$q_t + uq_x + vq_y = 0 \tag{58}$$

with the stream function related to the PV through

$$q = \mathit{\Delta}\psi + \beta y \tag{59}$$

which is the case where $L \to \infty$ in the SWQG or the case where there are no vertical derivatives in 3D QG. The relative vorticity, $q' = \mathit{\Delta}\psi$.

If we consider a PV patch which is initially circular so that

$$q' = q_0 \tag{60}$$

inside a disk of radius a and zero outside. We know that the velocity field is in the angular direction $\vec{u} = u_\theta\,\hat{\theta}$

$$u_\theta = \frac{q_0}{2}\begin{cases} r & r < a \\ \frac{a^2}{r} & r \geq a \end{cases} \tag{61}$$

Along particle trajectories, q is conserved so

$$\begin{aligned} q_{\text{after}} &= q_{\text{before}} \\ q'_{\text{after}} + \beta y_{\text{after}} &= q'_{\text{before}} + \beta y_{\text{before}} \\ q'_{\text{after}} - q'_{\text{before}} &= \beta y_{\text{before}} - \beta y_{\text{after}} \\ \Longrightarrow \quad \Delta q' &= -\beta\,\Delta y \\ \mathit{\Delta}\phi &= -\beta\,\Delta y \end{aligned} \tag{62}$$

Therefore the change in the relative PV of a particle is proportional to the negative of the change of its y-coordinate. I'm using ϕ to denote the change in the stream function because of the interchange of relative and potential vorticity.

This is an interesting problem to solve. Imagine an array of points, (X, Y) where $R = \sqrt{X^2 + Y^2}$, representing the initial (Lagrangian) coordinates of all the particles. They are mapped under the dynamics

$$\begin{aligned} \frac{dX}{dt} &= u(X, Y) = \vec{u}\cdot\hat{\imath} = -\frac{Y}{R}\,u_\theta(R) \\ \frac{dY}{dt} &= V(X, Y) = \vec{u}\cdot\hat{\jmath} = \frac{X}{R}\,u_\theta(R). \end{aligned} \tag{63}$$

This would be an exact mapping for all time if there was no β effect - but this effect changes the relative PV and so it changes ψ. For a small time, Δt we have

$$\begin{aligned} \Delta y &= \Delta t \, \frac{X}{R} \, u_\theta(R) \\ &= \frac{\Delta t \, q_0}{2} \begin{cases} X & R < a \\ \frac{a^2 X}{R^2} & R \geq a \end{cases} \end{aligned} \tag{64}$$

so the change in the stream function is given by

$$\Delta\phi = -\frac{\Delta t \, \beta \, q_0}{2} \begin{cases} X & R < a \\ \frac{a^2 X}{R^2} & R \geq a \end{cases} \tag{65}$$

Let $\phi = \frac{\Delta t \, \beta \, q_0}{2} \, \Phi$ so that

$$\Delta\Phi = \begin{cases} -X & R < a \\ -\frac{a^2 X}{R^2} & R \geq a \end{cases} \tag{66}$$

Let $\Phi = \cos(\theta)\rho(R)$ so that

$$\begin{aligned} \frac{1}{R}\frac{\partial}{\partial R}\left[R\frac{\partial\left(\rho\cos(\theta)\right)}{\partial R}\right] + \frac{1}{R^2}\frac{\partial^2}{\partial\theta^2}\left[\cos(\theta)\rho\right] = \cos(\theta) \begin{cases} -R & R < a \\ -\frac{a^2}{R} & R \geq a \end{cases} \\ \frac{1}{R}\frac{d}{dR}\left[R\frac{d\rho}{dR}\right] - \frac{\rho}{R^2} = \begin{cases} -R & R < a \\ -\frac{a^2}{R} & R \geq a \end{cases} \end{aligned} \tag{67}$$

Now let $s = \ln(R/a)$ so $R\frac{d}{dR} = \frac{d}{ds}$ and

$$\frac{d^2\rho}{ds^2} - \rho = \begin{cases} -a^3 e^{3s} & s < 0 \\ -a^3 e^{-s} & s \geq 0 \end{cases} \tag{68}$$

For $s < 0$ the solution is

$$\rho = -a^3\left[Ae^s + \frac{1}{8}e^{3s}\right] \tag{69}$$

while for $s > 0$

$$\rho = -a^3\left[Be^{-s} - \frac{1}{2}se^{-s}\right] \tag{70}$$

Now at $s = 0$ we want ρ and its derivative to match. Therefore

$$\begin{aligned} A + \frac{1}{8} &= B \\ A + \frac{3}{8} &= -B - \frac{1}{2} \end{aligned} \tag{71}$$

So $A = -\frac{4}{8}$, and $B = -\frac{3}{8}$ and the solution becomes

$$\rho = -\frac{a^3}{8} \begin{cases} e^{3s} - 4e^s & s < 0 \\ -\left(3 + 4s\right)e^{-s} & s \geq 0 \end{cases} \tag{72}$$

which is

$$\rho = -\frac{a^3}{8}\begin{cases} \left(\frac{R}{a}\right)^3 - 4\frac{R}{a} & R < a \\ -\left(3 + 4\ln\left(\frac{R}{a}\right)\right)\frac{a}{R} & R \geq a \end{cases} \tag{73}$$

So we conclude that inside the disk

$$\Phi = \frac{R\cos(\theta)}{8}\left[4a^2 - R^2\right] = \frac{X}{8}\left[4a^2 - \left(X^2 + Y^2\right)\right] \tag{74}$$

whereas outside the disk

$$\Phi = \frac{a^4\cos(\theta)}{8R}\left[3 + 4\ln\left(\frac{R}{a}\right)\right] = \frac{a^4 X}{8\left(X^2+Y^2\right)}\left[3 + 2\ln\left(\frac{X^2+Y^2}{a^2}\right)\right] \tag{75}$$

The actual induced stream function is proportional to Φ,

$$\phi = \frac{\Delta t \beta q_0}{2}\,\Phi. \tag{76}$$

The perturbation stream function is contoured in figure 7. Since the stream function pene-

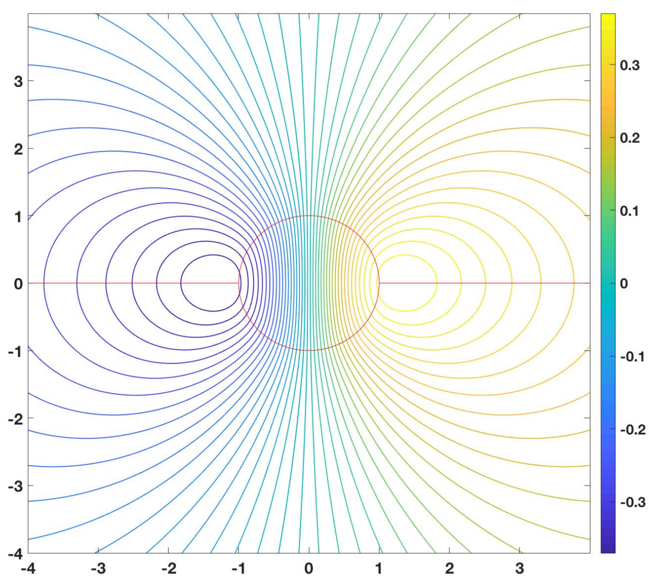

Figure 7: The induced stream function for a barotropic PV patch with $q_0 > 0$. The circular patch is shown in red. The original stream function is circularly symmetric and rotating counter clockwise. This perturbation stream function has positive Y-velocity within the patch so we expect the whole thing to be pushed upwards.

trates the boundary, the circular patch cannot remain circular in the presence of the β-effect.

The original stream function is circularly symmetric and rotating counter clockwise. This perturbation stream function has positive Y-velocity within the patch so we expect the whole thing to be pushed upwards.

Since the PV is changing everywhere in the domain, it is not sufficient to simply describe the effect of the induced velocity on the boundary of the patch - but it is instructive. The velocity of the original patch at the boundary of the patch is

$$u_* = \frac{q_0 a}{2} \tag{77}$$

Using interior stream function the upward component of induced velocity is

$$\begin{aligned}
\frac{\partial \phi}{\partial X} &= \left[\frac{\Delta t \beta q_0}{2}\right] \frac{1}{8} \left[4a^2 - R^2 - 2X^2\right] \\
\left.\frac{\partial \phi}{\partial X}\right|_{R=a} &= \left[\frac{\Delta t \beta q_0}{2}\right] \frac{a^2}{8} \left[3 - 2\cos^2(\theta)\right] \\
&= \left[\frac{\Delta t \beta q_0}{2}\right] \frac{a^2}{8} \left[2 - \cos(2\theta)\right] \\
&= \left[\frac{\Delta t \beta q_0 a^2}{2}\right] \left[\frac{1}{4} - \frac{\cos(2\theta)}{8}\right]
\end{aligned} \tag{78}$$

Notice that if we average this velocity around the circle we find

$$\frac{1}{2\pi} \int_0^{2\pi} \left.\frac{\partial \phi}{\partial X}\right|_{R=a} d\theta = \left[\frac{\Delta t \beta a}{4}\right] \left(\frac{q_0 a}{2}\right). \tag{79}$$

I think this is interesting because it says that the induced velocity is proportional to the original velocity (the amplitude) times a pre-factor which is proportional to the elapsed time, the size of the PV patch, and the strength of the β- effect.

Now computing the horizontal velocity at the patch we find

$$\begin{aligned}
-\frac{\partial \phi}{\partial Y} &= \left[\frac{\Delta t \beta q_0}{2}\right] \frac{XY}{4} \\
-\left.\frac{\partial \phi}{\partial Y}\right|_{R=a} &= \left[\frac{\Delta t \beta q_0}{2}\right] \frac{a^2 \sin(\theta)\cos(\theta)}{4} \\
-\left.\frac{\partial \phi}{\partial Y}\right|_{R=a} &= \left[\frac{\Delta t \beta q_0 a^2}{2}\right] \frac{\sin(2\theta)}{8}.
\end{aligned} \tag{80}$$

This velocity clearly averages to zero. However, we see that it is positive in the first and third quadrant and negative in the second and fourth quadrants.

One more simplification, let $\vec{U} = -\frac{\partial \phi}{\partial Y}\hat{\imath} + \frac{\partial \phi}{\partial X}\hat{\jmath}$. Define

$$\delta \equiv \frac{\Delta t \beta a}{4} \tag{81}$$

is the velocity fraction due to the time elapsed. Now using the definition (77) of u_* as the rotation rate of the patch at the boundary, we find that the induced velocity field at the boundary is

$$\vec{U} = \delta\, u_* \left[\hat{j} + \left(\frac{\sin(2\theta)\hat{\imath} - \cos(2\theta)\hat{j}}{2}\right)\right]. \tag{82}$$

Another way to look at the flow is to return to the potential inside the disk

$$\begin{aligned}\phi &= \frac{\Delta t\,\beta\,q_0 a^2}{2}\frac{X}{8}\left[4 - \frac{(X^2+Y^2)}{a^2}\right] \\ &= \delta\,u_*\,X\left[2 - \frac{(X^2+Y^2)}{2a^2}\right]\end{aligned} \tag{83}$$

and the vertical velocity is

$$\frac{\partial\phi}{\partial X} = \delta u_*\left[2 - \frac{(3X^2+Y^2)}{2a^2}.\right] \tag{84}$$

Now we can average this over the boundary, $R = a$ and find

$$\overline{\frac{\partial\phi}{\partial X}} = \delta u_*. \tag{85}$$

Alternatively, we can average over the area

$$\begin{aligned}\left\langle\frac{\partial\phi}{\partial X}\right\rangle &= \frac{1}{\pi a^2}\int_0^{2\pi}\int_0^a \delta u_*\left[2 - \frac{(3X^2+Y^2)}{2a^2}\right] R\,dR\,d\theta \\ &= \delta u_*\left[2 - \frac{1}{\pi}\int_0^{2\pi}\int_0^a \frac{3\cos^2(\theta)+\sin^2(\theta)}{2}\,\frac{R^3}{a^4}\,dR\,d\theta\right] \\ &= \delta u_*\left[2 - \frac{1}{\pi}\times 2\pi\times\frac{1}{2}(3+1)\times\frac{1}{2}\int_0^1 u^3\,du\right] \\ &= 2\delta u_*\left[1 - \frac{1}{4}\right] \\ &= \frac{3}{2}\delta u_*\end{aligned} \tag{86}$$

meaning the area averaged velocity is 3/2 the boundary averaged velocity. Now we can split the potential up so that the area averaged velocity is separated from the rest of the potential, thereby

$$\begin{aligned}\phi &= \delta u_*\,X\left[\frac{3}{2} + \frac{a^2 - (X^2+Y^2)}{2a^2}\right] \\ &= \delta u_*\,X\left[\frac{3}{2} + \frac{a^2 - R^2}{2a^2}\right]\end{aligned} \tag{87}$$

For completeness, we record the induced potential outside the patch

$$
\begin{aligned}
\phi &= \frac{\Delta t \beta q_0}{2} \frac{a^4 X}{8\left(X^2+Y^2\right)}\left[3+2\ln\left(\frac{X^2+Y^2}{a^2}\right)\right] \\
&= \delta u_* X\left\{\frac{a^2}{R^2}\left[\frac{3}{2}+\ln\left(\frac{R^2}{a^2}\right)\right]\right\} \\
&= \delta u_* X\left[\frac{3}{2}\left(\frac{a^2-R^2}{R^2}\right)+\left(\frac{a^2}{R^2}\right)\ln\left(\frac{R^2}{a^2}\right)+\frac{3}{2}\right]
\end{aligned} \tag{88}
$$

The stream function in the frame of reference moving with the mean speed of the patch is simply

$$\phi - \frac{3\delta u_* X}{2} \tag{89}$$

which is evident from the functional forms we've written above. It is also clear that this stream function vanishes at the boundary, $R = a$.

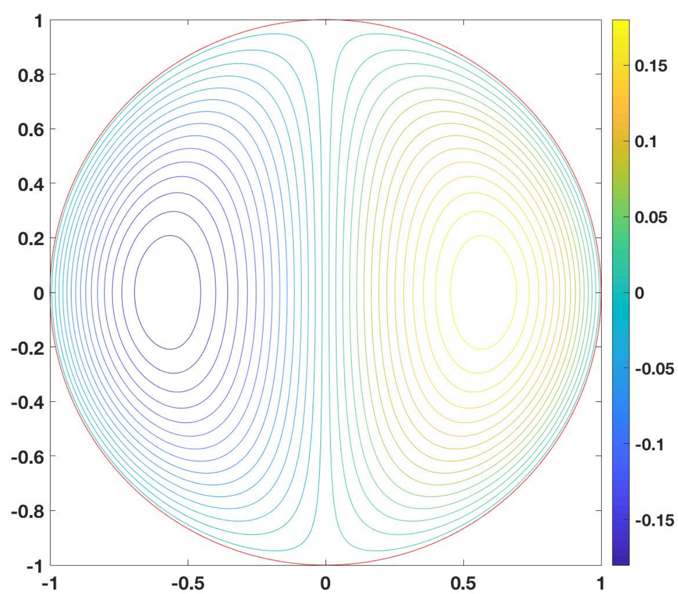

Figure 8: The induced stream function for a barotropic PV patch with $q_0 > 0$, in the frame of reference moving with the average vertical speed of the patch. The circular patch is shown in red and the contours are only plotted within the patch. The flow is everywhere upward along the y-axis. This circulation looks like Hill's vortex.